Clathrin-independent endocytosis of ErbB2 in geldanamycin-treated human breast cancer cells

Daniel J. Barr, Anne G. Ostermeyer-Fay, Rachel A. Matundan and Deborah A. Brown*

Department of Biochemistry and Cell Biology, Stony Brook University, Stony Brook, NY 11794-5215, USA

*Author for correspondence (e-mail: deborah.brown@sunysb.edu)

Accepted 25 June 2008
Journal of Cell Science 121, 3155-3166 Published by The Company of Biologists 2008
doi:10.1242/jcs.020404

Summary

The epidermal growth factor (EGF)-receptor family member ErbB2 is commonly overexpressed in human breast cancer cells and correlates with poor prognosis. Geldanamycin (GA) induces the ubiquitylation, intracellular accumulation and degradation of ErbB2. Whether GA stimulates ErbB2 internalization is controversial. We found that ErbB2 was internalized constitutively at a rate that was not affected by GA in SK-BR-3 breast cancer cells. Instead, GA treatment altered endosomal sorting, causing the transport of ErbB2 to lysosomes for degradation. In contrast to earlier work, we found that ErbB2 internalization occurred by a clathrin- and tyrosine-kinase-independent pathway that was not caveolar, because SK-BR-3 cells lack caveolae. Similar to cargo of the glycosylphosphatidylinositol (GPI)-anchored protein-enriched early endosomal compartment (GEEC) pathway, internalized ErbB2 colocalized with cholera toxin B subunit, GPI-anchored proteins and fluid, and was often seen in short tubules or large vesicles. However, in contrast to the GEEC pathway in other cells, internalization of ErbB2 and fluid in SK-BR-3 cells did not require Rho-family GTPase activity. Accumulation of ErbB2 in vesicles containing constitutively active Arf6-Q67L occurred only without GA treatment; Arf6-Q67L did not slow transport to lysosomes in GA-treated cells. Further characterization of this novel clathrin-, caveolae- and Rho-family-independent endocytic pathway might reveal new strategies for the downregulation of ErbB2 in breast cancer.

Supplementary material available online at
http://jcs.biologists.org/cgi/content/full/121/19/3155/DC1

Key words: Non-clathrin endocytosis, Membrane traffic, Receptor tyrosine kinase, Receptor downregulation, Arf6, Rho-family GTPase, HER2

Introduction

ErbB2 is a member of the ErbB family of receptor tyrosine kinases, which also includes the epidermal growth factor receptor (EGFR or ErbB1) (Yarden and Sliwkowski, 2001). ErbB2 is the preferred heterodimerization partner of the other ErbB family members and enhances their signaling, although it has no known ligand of its own (Graus-Porta et al., 1997; Lenferink et al., 1998). ErbB2 is overexpressed in 20-30% of human breast cancers and is associated with poor prognosis (Slamon et al., 1987). Thus, ErbB2 downregulation is an important goal in the treatment of breast cancer.

Unlike other ErbB proteins, ErbB2 binds constitutively to the chaperone Hsp90 (Xu et al., 2001). The ansamycin antibiotic geldanamycin (GA) releases Hsp90 from its client proteins, destabilizing them (Hohfeld et al., 2001; Richter and Buchner, 2001). Following release of Hsp90 from ErbB2, both Hsp70 and the co-chaperone E3 ubiquitin-protein ligase CHIP (CHIP) are recruited to the receptor (Citri et al., 2004; Xu et al., 2002; Zhou et al., 2003). CHIP ubiquitylates ErbB2, leading to its intracellular accumulation and degradation with a half life ($t_{1/2}$) of about 2 hours. The GA analog 17-allylamino, 17-demethoxygeldanamycin is in clinical trials for the treatment of ErbB2-dependent breast cancer (Sharp and Workman, 2006).

The step(s) at which GA affects ErbB2 endocytic transport remain controversial. One group found that interactions of the cytoplasmic domain of ErbB2 with unknown binding partner(s) normally stabilize the protein at the plasma membrane and make it resistant to internalization (Hommelgaard et al., 2004; Lerdrup et al., 2007). They found that GA overcame this effect and stimulated ErbB2 internalization (Lerdrup et al., 2006). By contrast, a second group found that ErbB2 was constitutively internalized, but normally recycled efficiently so that most of the protein was on the plasma membrane at steady state (Austin et al., 2004). In their hands, GA did not affect internalization of ErbB2, but altered sorting in endosomes, reducing recycling and leading to accumulation inside multivesicular bodies (MVBs) (Austin et al., 2004).

Early reports suggested that, after release of Hsp90, ErbB2 is degraded by proteasomes, rather than in lysosomes (Citri et al., 2002; Mimnaugh et al., 1996; Way et al., 2004). However, later work suggested that ErbB2 is transported through early and late endosomes for degradation in lysosomes. Internalized ErbB2 colocalizes with transferrin (Tf) and is present in internal vesicles inside MVBs, suggesting transport to lysosomes for degradation (Austin et al., 2004).

ErbB2 degradation was initially reported to be insensitive to lysosomal inhibitors (Citri et al., 2002; Mimnaugh et al., 1996; Way et al., 2004). However, later work showed that a cytoplasmic-domain fragment is cleaved from Erb2 in GA-treated cells, rendering the protein undetectable by antibodies previously used on blots (Tikhomirov and Carpenter, 2000; Tikhomirov and Carpenter, 2001). Use of an extracellular-domain-specific antibody showed that lysosomal inhibitors stabilize a clipped 135 kDa form of ErbB2 in GA-treated cells (Tikhomirov and Carpenter, 2000). Proteasome inhibitors were later shown to retard ErbB2 degradation in GA-treated cells indirectly, by inhibiting internalization (Lerdrup et al., 2006). Even intact ErbB2 was found to be internalized and degraded in lysosomes upon GA treatment (Lerdrup et al., 2006).

In this paper, we examined the internalization of ErbB2 in GA-treated breast cancer cells. We found that GA did not affect the

rate of ErbB2 internalization. In contrast to a previous report (Austin et al., 2005), we found that ErbB2 was internalized by a clathrin-independent pathway. ErbB2 was internalized by a similar pathway in transfected COS-7 cells, showing the generality of this finding.

Cells exhibit a number of clathrin-independent endocytic pathways (Conner and Schmid, 2003; Kirkham and Parton, 2005). Endocytosis in caveolae requires caveolin-1 and dynamin, and tyrosine-kinase activity (Kirkham and Parton, 2005). A similar pathway, which is found in cells that lack caveolin-1, also requires tyrosine-kinase activity (Damm et al., 2005). CHO cells internalize glycosylphosphatidylinositol (GPI)-anchored proteins, but not transmembrane proteins, into GPI-anchored protein-enriched early endosomal compartments (GEECs), which additionally contain fluid-phase markers (Sabharanjak et al., 2002; Kalia et al., 2006; Chadda et al., 2007; Kumari and Mayor, 2008).

Cholera toxin B subunit (CtxB) binds the ganglioside GM1 and can be internalized by several different means, including the clathrin-mediated and caveolar pathways (Lencer and Saslowsky, 2005; Sandvig and Van Deurs, 2002). At least in some cells, most CtxB is taken up into clathrin- and caveolin-independent carriers (CLICs), which have a distinctive tubular and ring-like morphology (Kirkham and Parton, 2005). These also contain internalized GPI-anchored proteins and fluid, suggesting that they are the same as GEECs (Kirkham et al., 2005).

In contrast to CHO cells, HeLa cells do not have a dedicated pathway for internalization of GPI-anchored proteins. In these cells, both GPI-anchored and transmembrane proteins follow a non-clathrin, non-caveolar endocytic pathway that is regulated by Arf6 (Naslavsky et al., 2003; Naslavsky et al., 2004). Constitutively active Arf6-Q67L causes cargo of this pathway to accumulate in enlarged vacuoles (Naslavsky et al., 2003; Naslavsky et al., 2004). The swollen vacuoles induced by Arf6-Q67L were proposed to represent an intermediate compartment, upstream of early endosomes (Naslavsky et al., 2003). Arf6-Q67L slows exit from this compartment, leading to swelling. As expected from this model, Arf6-Q67L blocked the normal transport of GPI-anchored proteins to Rab5-positive early endosomes and then on to lysosomes, and also blocked degradation of cargo that accumulated in the Arf6-Q67L-positive vacuoles (Naslavsky et al., 2003).

By contrast, the GEEC pathway in CHO cells is not regulated by Arf6 (Kalia et al., 2006). However, both the Arf6-regulated and GEEC pathways rapidly merge with the ‘classical’ clathrin-mediated pathway at the level of Rab5-positive early endosomes (Kalia et al., 2006; Naslavsky et al., 2003).

Several clathrin-independent endocytic pathways require Rho-family GTPase activity (Mayor and Pagano, 2007). For instance, RhoA is required for the uptake of interleukin-2 receptor in T cells (Lamaze et al., 2001) and of albumin in CHO cells (Cheng et al., 2006). Cdc42 is required for efficient fluid-phase uptake in immature dendritic cells (Garrett et al., 2000) and for the GEEC pathway in CHO cells (Chadda et al., 2007; Sabharanjak et al., 2002).

Here, we showed that, in SK-BR-3 cells both with and without GA treatment, ErbB2 was internalized via a non-clathrin, non-caveolar pathway together with a GPI-anchored protein, CtxB, and fluid. In GA-treated cells, ErbB2 was then transported to lysosomes for degradation. Although ErbB2 accumulated in Arf6-Q67L-positive vacuoles in the absence of drug treatment, Arf6-Q67L did not slow ErbB2 transport to lysosomes in GA-treated cells. Endocytosis of ErbB2 and fluid in SK-BR-3 cells did not require Rho-family GTPase function.

Results

ErbB2 internalization in GA-treated SK-BR-3 cells is independent of clathrin

Immunofluorescence microscopy showed high levels of ErbB2 on the surface of SK-BR-3 cells (Fig. 1A), as reported previously (Austin et al., 2004; Hommelgaard et al., 2004). Also as reported (Austin et al., 2004; Hommelgaard et al., 2004), fluorescein-conjugated surface-bound anti-ErbB2 antibodies (Fl-anti-ErbB2) did not greatly affect ErbB2 localization (Fig. 1B). By contrast, after 2-3 hours of GA treatment, ErbB2 was abundant in intracellular punctae, whereas surface localization was reduced (Fig. 1C).

To determine the role of the clathrin pathway in ErbB2 endocytosis in GA-treated cells, we first used chlorpromazine (CPZ), a cationic amphiphile that inhibits this pathway (Wang et

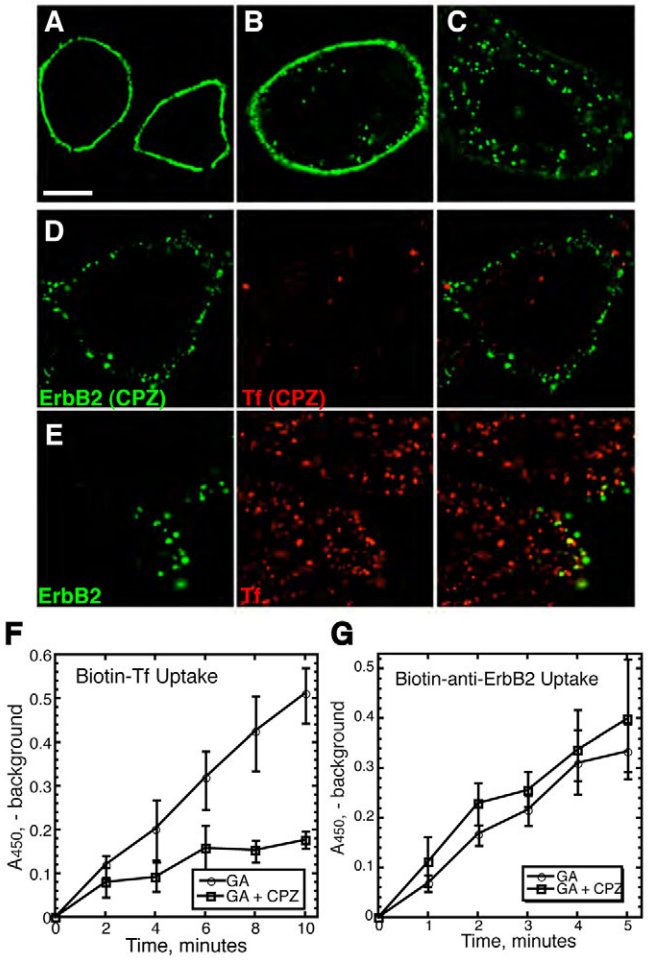

Fig. 1. Effect of bound antibodies, GA and CPZ on ErbB2 localization in SK-BR-3 cells. (A) ErbB2 in fixed, permeabilized cells detected by immunofluorescence. (B) Cells were warmed for 2 hours after binding Fl-anti-ErbB2 before fixation. (C) Cells were treated with GA for 2 hours before detecting ErbB2 by immunofluorescence. (D,E) Cells were pre-treated for 45 minutes at 37°C with GA, with (D) or without (E) 12 μg/ml CPZ, before binding anti-ErBb2 antibodies (left, green) and Alexa-Fluor-594-Tf (middle, red) for 1 hour on ice and warming for 2 minutes with the same drugs. Cells were acid-washed and processed for immunofluorescence, detecting ErbB2 with the Alexa-Fluor-488 Zenon mouse IgG labeling kit. Merged images are shown on the right. Scale bar: 10 μm. (F,G) Internalization of biotinylated Tf (F) or biotinylated anti-ErbB2 antibodies (G) was measured by CELISA after treatment with GA (circles) or both GA and CPZ (squares). Values shown are the mean ± s.e.m. of three experiments.

al., 1993). CPZ efficiently inhibited the uptake of Alexa-Fluor-594-conjugated Tf, but did not block ErbB2 internalization (Fig. 1D,E). After CPZ treatment, structures containing internalized ErbB2 sometimes had a tubular morphology (D.J.B., unpublished), which might have resulted from the ability of CPZ to induce membrane curvature (Lange and Steck, 1984). Cell-based enzyme linked immunosorbent assay (CELISA) showed that CPZ inhibited the uptake of biotinylated Tf (Fig. 1F), but did not affect the internalization of biotinylated anti-ErbB2 antibodies (Fig. 1G).

We next determined whether, soon after internalization, ErbB2 colocalized with markers of the clathrin pathway. Most ErbB2-positive punctae did not label for rhodamine-conjugated Tf (Rh-Tf) (Fig. 1 and Fig. 2A,E,H). By contrast, internalized EGFR and Tf colocalized extensively with each other (Fig. 2B,H). ErbB2 did not colocalize significantly with clathrin (Fig. 2C,F), whereas EGFR did (Fig. 2D,G). ErbB2-positive structures often had a distinctive morphology (either short tubules, or round structures with visible lumens), captured most clearly in favorable epifluorescence images (Fig. 2A,E). These images also showed that ErbB2-positive structures remained closer to the plasma membrane than Rh-Tf-positive structures after 5 minutes of internalization. These results showed that ErbB2 did not colocalize with markers of the clathrin-dependent internalization pathway soon after internalization in GA-treated cells, and suggested that it was internalized by a different mechanism.

Eps15 associates with the clathrin coat and is required for clathrin-mediated uptake (Conner and Schmid, 2003). Dynamins mediate endocytic vesicle scission and are required for both clathrin-mediated and caveolar endocytosis (Conner and Schmid, 2003). Dominant-negative forms of Eps15 and dynamin-1 had similar effects in GA-treated SK-BR-3 cells: Rh-Tf uptake was inhibited, whereas ErbB2 internalization was still detected (Fig. 3A,B). Results were quantified (Fig. 3C,D) by counting the number of cells that were positive or negative for internalization of ErbB2 and Tf.

Together, these results showed that ErbB2 was internalized primarily by a clathrin-independent mechanism in GA-treated SK-BR-3 cells. We next compared ErbB2 internalization to other clathrin-independent endocytic pathways.

ErbB2 internalization does not require tyrosine-kinase activity

Because SK-BR-3 cells do not express caveolin-1 and lack caveolae (Hommelgaard et al., 2004), ErbB2 cannot be internalized by caveolar endocytosis in these cells. However, a ‘caveolar-like’ pathway that is followed by cargoes that are normally internalized in caveolae, can exist in cells that lack caveolae. Endocytosis by this pathway is inhibited by the tyrosine-kinase inhibitor genistein (Damm et al., 2005; Sharma et al., 2004). We next determined whether ErbB2 internalization was sensitive to genistein. As a positive control, we verified that genistein inhibited the EGF-induced stimulation of tyrosine-kinase activity and the internalization of tyrosine-phosphorylated substrates. SK-BR-3 cells express EGFR, although at lower levels than ErbB2 (Beerli et al., 1995). In untreated serum-starved cells (D.J.B., unpublished) and in cells treated with GA alone (Fig. 4A, middle), anti-phosphotyrosine staining was usually dim and was largely restricted to the plasma membrane. However, after EGF treatment, internal punctae stained brightly with anti-phosphotyrosine antibodies (Fig. 4B, middle). As previously reported (Haslekås et al., 2005; Wang et al., 1999), EGF did not alter the distribution of ErbB2 (Fig. 4B, top). As expected, both ErbB2 and tyrosine-phosphorylated

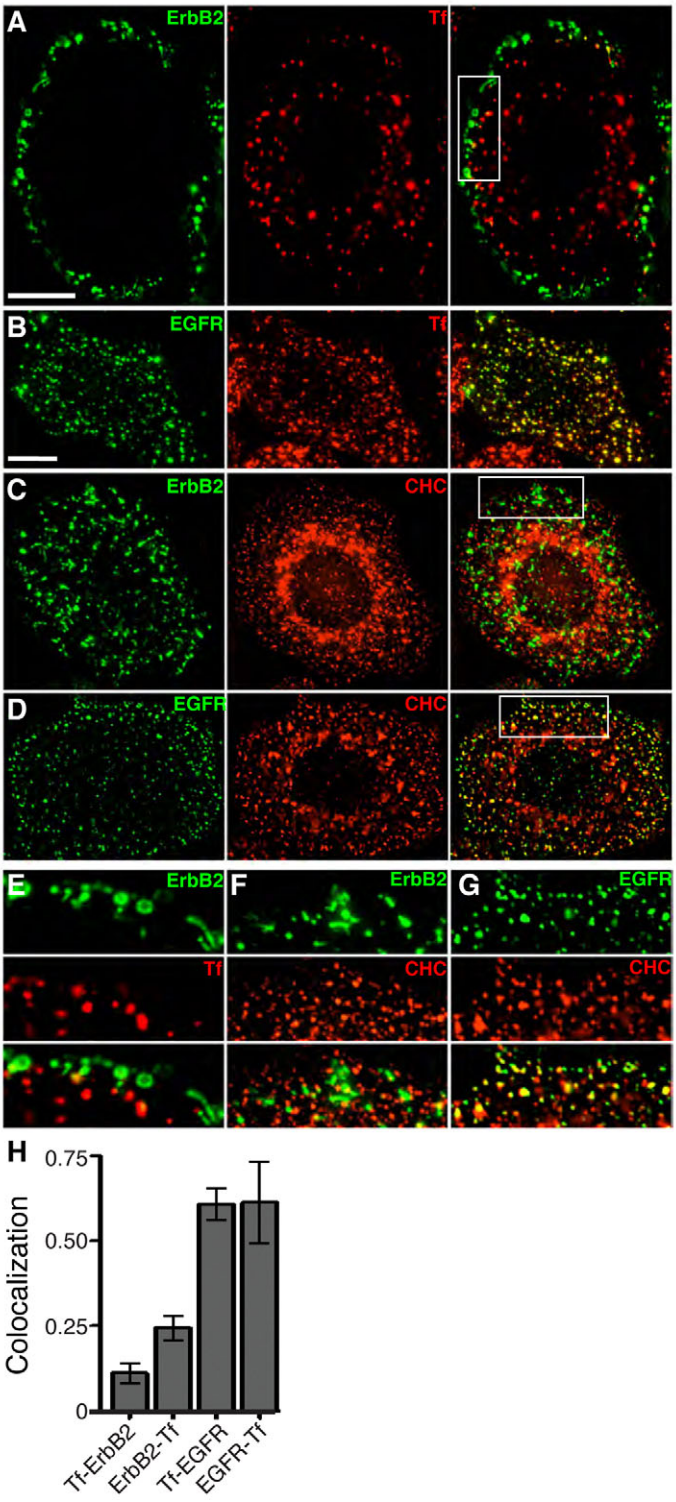

Fig. 2. Localization of internalized ErbB2, Rh-Tf, EGFR and clathrin. SK-BR-3 cells were pretreated with GA for 1 hour before binding Fl-anti-ErbB2 (A,C,E,F) or Fl-anti-EGFR (B,D,G) and warming for 5 minutes (with Rh-Tf in A,B and E) before acid washing and immunofluorescence analysis. (C,D) Clathrin heavy chain (CHC, red) was detected by immunofluorescence. (E-G) High-magnification views of the boxed regions in A,C and D, respectively. Right-hand panels in A-D and bottom panels in E-G show merged images. (A) Epifluorescence images. All other panels show maximum-intensity projections of deconvolved *z*-stacks. Scale bars: 10 μm (bar in B applies to B-D). (H) Quantification of colocalization of Rh-Tf with ErbB2 or EGFR in cells treated as in A,B, except that internalization was for 2 minutes.

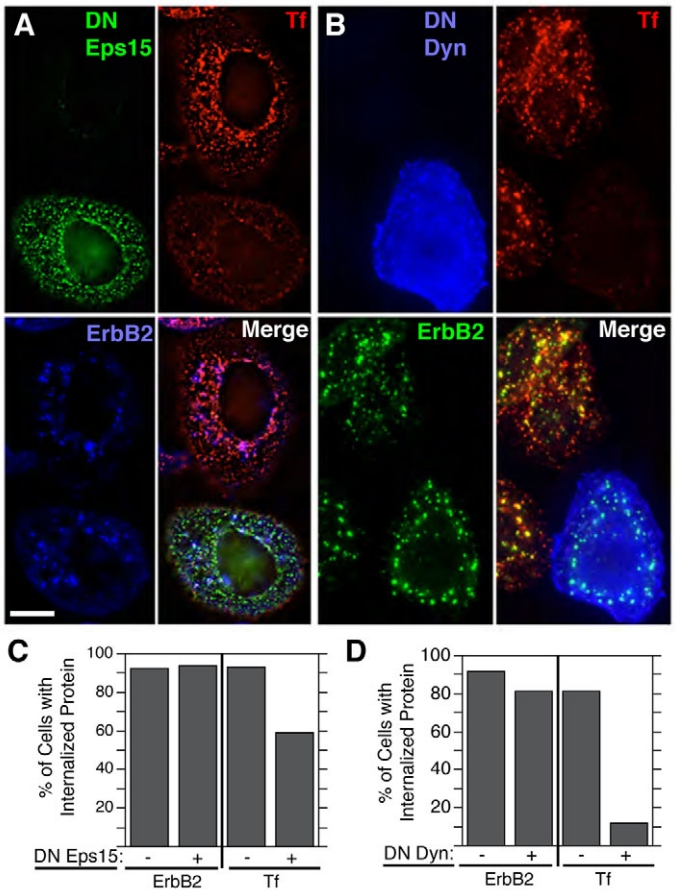

Fig. 3. Dominant-negative forms of Eps15 and dynamin inhibit internalization of Rh-Tf but not ErbB2. SK-BR-3 cells transfected with EGFP–DN-Eps15 (A,C) or HA–DN-dynamin-1 (B,D) were pretreated with GA for 2 hours before binding unlabeled anti-ErbB2 antibodies (A,C) or Fl-anti-ErbB2 antibodies (B,D). Cells were then warmed for 30 minutes with Rh-Tf, fixed and permeabilized. (A,B) EGFP–DN-Eps15 (A, green) or HA–DN-dynamin (B, blue) are shown with Rh-TF and ErbB2 in deconvolved images, each from a *z*-stack of a field in which one cell expressed DN-Eps15 (A) or DN-dynamin (B). ErbB2 was detected with Alexa-Fluor-350 goat anti-mouse antibodies (A, blue; C) or by fluorescein fluorescence (B, green; D). Scale bar: 10 μm. (C,D) Internalization of ErbB2 and Rh-Tf in cells expressing EGFP–DN-Eps15 (C) or HA–DN-dynamin (D) (+), and untransfected cells on the same coverslips (–). Cells showing at least three intracellular punctae were scored positive. Numbers shown are averages of two experiments (counting at least 100 transfected and 100 untransfected cells in each experiment), the data from which varied by <10%.

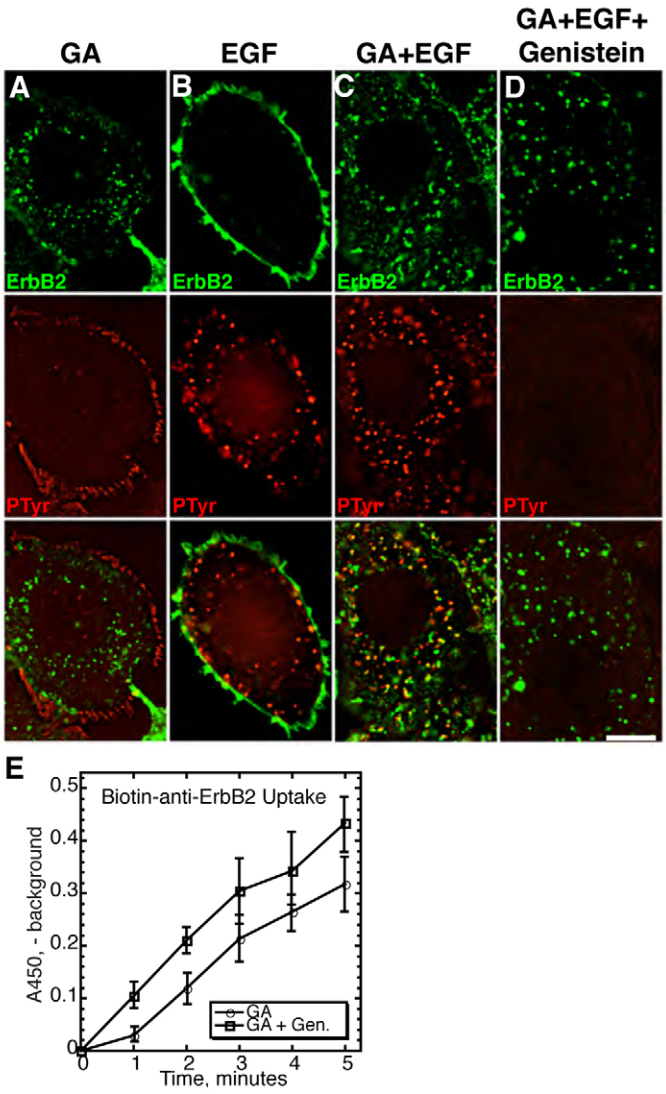

Fig. 4. Genistein inhibits EGF-stimulated tyrosine-kinase activity but not ErbB2 internalization. SK-BR-3 cells were serum-starved overnight, treated as described below for the individual panels, fixed and permeabilized. Cells were treated with: (A) GA for 2 hours; (B) 100 ng/ml EGF for 10 minutes; (C) GA for 2 hours, with 100 ng/ml EGF added for the last 10 minutes; and (D) 100 μg/ml genistein for 1 hour, then GA added for another 2 hours and 100 ng/ml EGF added for the last 10 minutes. Deconvolved images from *z*-stacks are shown. ErbB2 (green, top) and phosphotyrosine (P-Tyr; red, middle) were detected by immunofluorescence. Bottom: merged images. Scale bar: 10 μm. (E) SK-BR-3 cells were pretreated with GA (circles) or GA + 100 μg/ml genistein (squares) for 45 minutes before binding biotinylated anti-ErbB2 antibodies and warming for 0-5 minutes. Internalized antibodies were quantified by CELISA. Values shown are the mean ± s.e.m. of three experiments.

substrates were internalized in cells treated with EGF and GA together (Fig. 4C). Genistein treatment blocked tyrosine phosphorylation in cells treated with EGF and GA, but ErbB2 internalization remained robust (Fig. 4D). CELISA analysis showed that genistein did not inhibit, and in fact slightly stimulated, ErbB2 internalization (Fig. 4E). This is consistent with a report that ErbB2 internalization in GA-treated cells does not require its tyrosine-kinase activity (Xu et al., 2001), and also shows that no other tyrosine kinase is required.

ErbB2 colocalizes with Alexa-Fluor-594-CtxB, GPI-anchored proteins and a fluid-phase marker immediately after internalization

To determine whether ErbB2 was internalized by a GEEC- and/or CLIC-like pathway (Kalia et al., 2006; Kirkham and Parton, 2005; Sabharanjak et al., 2002), we examined markers of those pathways. After 5 minutes of uptake in GA-treated SK-BR-3 cells, internalized ErbB2 colocalized extensively with co-internalized Alexa-Fluor-594-conjugated CtxB, GPI-anchored placental alkaline phosphatase (PLAP) and the fluid-phase marker FluoroRuby dextran (Fig. 5A-D). Quantification of the colocalization of ErbB2 with CtxB, PLAP and Thy1 (another GPI-anchored protein) is shown in Fig. 5E. Slightly higher colocalization of ErbB2 with Thy1 than with PLAP might be a result of more-efficient acid stripping of anti-Thy1 than anti-PLAP antibodies from the cell surface.

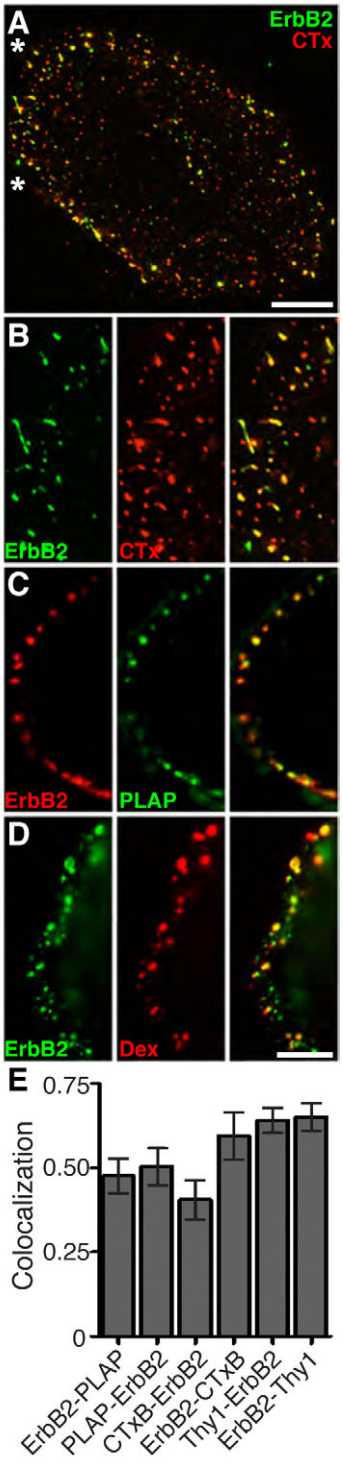

Fig. 5. Internalized ErbB2 colocalizes with Alexa-Fluor-594-CtxB, GPI-anchored proteins and dextran in GA-treated SK-BR-3 cells. Cells were pretreated with GA for 1 hour, subjected to antibody and/or toxin binding, warmed for 5 minutes, acid-stripped and fixed. (A) Fl-anti-ErbB2 (green) and Alexa-Fluor-594-CtxB (0.5 μg/ml; red) were bound to cells. A merged maximum-intensity projection image of a deconvolved *z*-stack is shown. Asterisks delimit the region shown enlarged in B (ErbB2, left; Alexa-Fluor-594-CtxB, middle; merged image, right). (C) Fl-anti-PLAP Fab fragments and Rh-anti-ErbB2 antibodies were bound to cells. A deconvolved image from a *z*-stack, showing part of the edge of one cell, is shown. ErbB2, left; PLAP, middle; merged image, right. (D) Fl-anti-ErbB2 was bound to cells, which were warmed with 1 mg/ml FluoroRuby dextran. An epifluorescence image, showing part of the edge of one cell, is shown. ErbB2, left; dextran, middle; merged image, right. Scale bars: 10 μm (A); 5 μm (D; applies to B-D). (E) Colocalization of ErbB2 and CtxB, or ErbB2 and PLAP, in cells treated as in A-C (except that internalization was for 2 minutes) was quantified. To measure the colocalization of ErbB2 and Thy1.1, SK-BR-3 cells transfected with Thy1.1 were treated with GA for 1 hour. Fl-anti-ErbB2 and Alexa-Fluor-594-anti-Thy1 Fab fragments were bound on ice, and cells warmed for 2 minutes. Residual surface-bound antibodies were acid-stripped before fixation, visualization and quantification.

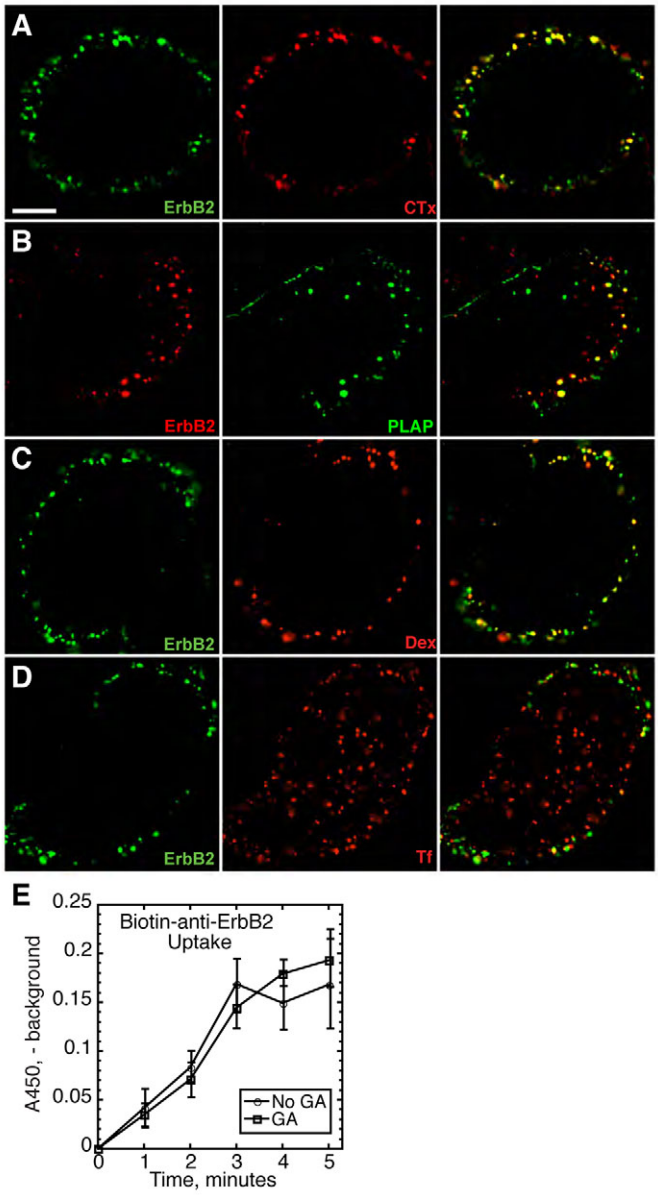

Fig. 6. Internalized ErbB2 colocalizes with CtxB, GPI-anchored proteins and dextran in SK-BR-3 cells without GA. (A-D) Cells were subjected to antibody and/or toxin binding on ice for 1 hour, warmed for 2 minutes, acid-stripped and fixed. (A) Fl-anti-ErbB2 and Alexa-Fluor-594-CtxB (0.5 μg/ml) were bound to cells. (B) Fl-anti-PLAP Fab fragments and Rh-anti-ErbB2 antibodies were bound to cells. (C) Fl-anti-ErbB2 was bound to cells, which were warmed with 1 mg/ml FluoroRuby dextran. (D) Fl-anti-ErbB2 and Rh-Tf were bound to cells. (A-D) Deconvolved images from *z*-stacks are shown. ErbB2, left; CtxB, PLAP, dextran or Tf, middle; merged images, right. Scale bar: 10 μm. (E) Internalization of biotinylated anti-ErbB2 antibodies was measured by CELISA in cells treated with (squares) or without (circles) GA. Values shown are the mean ± s.e.m. of three experiments.

These observations suggest that ErbB2 is internalized by a pathway that is similar to the GEEC pathway (Kalia et al., 2006; Kirkham et al., 2005; Sabharanjak et al., 2002). Also in common with the GEEC pathway, the PI(3) kinase inhibitor LY294002 did not inhibit ErbB2 internalization (supplementary material Fig. S1).

GA treatment does not affect ErbB2 internalization

We next wanted to determine whether ErbB2 was internalized by the same pathway in the absence of GA. ErbB2 that internalized without GA for 2 or 5 minutes was indistinguishable from that internalized in drug-treated cells (D.J.B., unpublished). As in GA-treated cells (Fig. 5), newly internalized ErbB2 colocalized with PLAP, CtxB and dextran in cells that were not treated with the drug (Fig. 6A-D). Furthermore, in agreement with a previous report (Austin et al., 2004), CELISA showed that the presence of GA did not affect the rate of ErbB2 internalization (Fig. 6E). We conclude

that GA does not affect the rate of ErbB2 internalization or the endocytic pathway that is followed.

Internalization of ErbB2 and fluid in SK-BR-3 cells does not require Rho-family GTPase activity

We used *C. difficile* toxin B, a Rho-family GTPase inhibitor (Jank et al., 2007), to determine whether a member of this family regulated fluid-phase uptake or ErbB2 endocytosis in SK-BR-3 cells. Growth factors stimulate macropinocytosis and fluid-phase uptake through the activation of Rac (Bryant et al., 2007; Ridley et al., 1992; Schnatwinkel et al., 2004). To avoid possible confounding effects of growth-factor-stimulated macropinocytosis, we performed these studies in serum-starved cells. Newly internalized ErbB2 colocalized with fluid, PLAP and CtxB in serum-starved cells, showing that serum starvation did not alter the internalization pathway of ErbB2 (supplementary material Fig. S2).

As expected, *C. difficile* toxin B completely abolished stress fiber formation, a process that requires RhoA function (Pellegrin and Mellor, 2007) (Fig. 7A). The toxin also drastically altered cell morphology, presumably by inhibiting Rho-family proteins that regulate the actin cytoskeleton (Fig. 7B,C). (Cell-surface ErbB2 was visualized in these cells after dextran internalization, serving as a marker of cell shape.) Nevertheless, the toxin did not greatly affect internalization of ErbB2 or a fluid-phase marker, as judged by fluorescence microscopy and biochemical internalization assays (Fig. 7B-E). As expected from this result, dominant-negative forms of Cdc42 and RhoA did not block ErbB2 internalization (supplementary material Fig. S3). We conclude that Rho-family proteins are not required for ErbB2 internalization in SK-BR-3 cells. This property distinguishes the internalization pathway that is followed by ErbB2, fluid and GPI-anchored proteins in these cells from the GEEC pathway described in CHO cells (Sabharanjak et al., 2002).

ErbB2 is transported to early and late endosomes and is degraded in lysosomes in GA-treated cells

ErbB2 colocalized significantly with Rh-Tf at long internalization times (Fig. 8A). This suggested that ErbB2 merged with the classical endocytic pathway following internalization. Consistently, and in agreement with earlier work (Austin et al., 2004), after 2 hours of GA treatment, ErbB2 colocalized with the early endosome markers EEA1 and Rab5 (Fig. 8B,C), and accumulated inside enlarged endosomes that were present in cells expressing constitutively active Rab5Q79L (Stenmark et al., 1994) (Fig. 8D). ErbB2 was sometimes detected inside structures that were surrounded with EEA1 in an irregular form. That is, EEA1 did not have a uniform distribution on these endosomes but was concentrated in sub-regions that appeared thicker than a single membrane and sometimes protruded from the endosome surface (Fig. 8B). These structures are probably the same as immature CD63-negative MVBs, which are surrounded by Tf-positive tubules, in which ErbB2 was detected in the interior vesicles by electron microscopy after 3 hours of GA treatment (Austin et al., 2004). The irregular appearance of EEA1 might reflect its localization in these tubules. After prolonged GA treatment, ErbB2 also colocalized with the late endosome markers GFP-Rab7 and CD63 (Fig. 9). Austin et al. reported little colocalization of ErbB2 with late endosome markers after 3 hours of GA treatment (Austin et al., 2004). This might have resulted from rapid degradation following delivery to lysosomes. As expected, colocalization of ErbB2 with LAMP1 was enhanced when lysosomal proteases were inhibited with leupeptin (Fig. 9D).

Lysosomotropic amines such as chloroquine raise the pH of endosomes and lysosomes and induce their swelling. Some groups have found that these compounds inhibit transport from early to late endosomes (Gu and Gruenberg, 2000), whereas others have found no such effect (Vonderheit and Helenius, 2005). ErbB2 colocalized with CD63 and LAMP1 in cells treated with GA and chloroquine (supplementary material Fig. S4), showing that

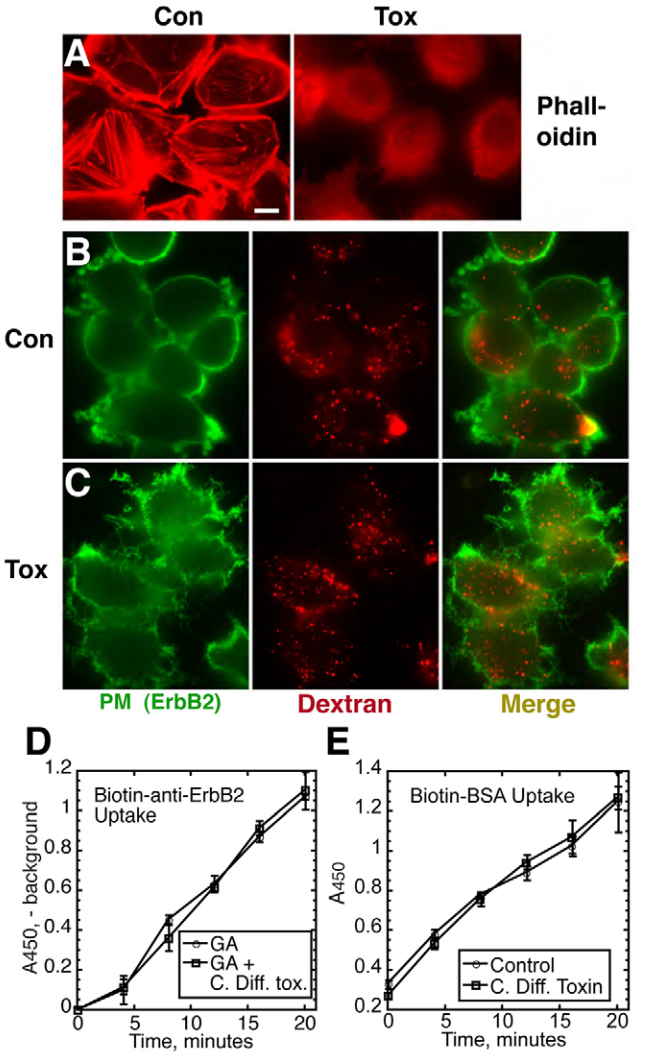

Fig. 7. *C. difficile* toxin B does not inhibit internalization of ErbB2 or fluid in SK-BR-3 cells. (A) SK-BR-3 cells grown for 48 hours on poly-Lys-coated coverslips were left untreated (Con) or were treated for 2 hours with 0.5 μg/ml *C. difficile* toxin B (Tox), fixed, permeabilized and incubated with rhodamine phalloidin (4 U/ml). Stress fibers were seen in about half of the control cells and <1% of treated cells. (B,C) Serum-starved SK-BR-3 cells on poly-Lys-coated coverslips were left untreated (B) or were treated for 2 hours with 0.5 μg/ml *C. difficile* toxin B (C) before addition of FluoroRuby dextran (1 mg/ml) for 10 minutes. After fixation, surface morphology was visualized with anti-ErbB2 antibodies and green secondary antibodies. PM, plasma membrane. Scale bar: 10 μm. (D,E) Internalization of biotinylated anti-ErbB2 antibodies (D) or biotinylated BSA (E) was measured by CELISA in serum-starved SK-BR-3 cells treated with GA (D, circles), GA + *C. difficile* toxin B (D, squares), *C. difficile* toxin alone (E, squares) or left untreated (E, circles) as described in the Materials and Methods. Where appropriate, cells were pre-incubated with *C. difficile* toxin B (0.5 μg/ml) for 2 hours at 37°C with the addition of GA for the last 45 minutes. Values shown are the mean ± s.e.m. of three experiments.

transport of ErbB2 to late endosomes and lysosomes did not require acidic luminal pH in these organelles. Together, these results showed that, after internalization by a clathrin-independent pathway, ErbB2 is transported to early and late endosomes, and then to lysosomes for degradation.

To test this possibility further, we examined ErbB2 degradation in GA-treated SK-BR-3 cells by western blotting. Consistent with an earlier report (Tikhomirov and Carpenter, 2000), a fragment of about 135 kDa that reacted with extracellular-domain-specific anti-ErbB2 antibodies accumulated in lysates of cells treated with GA and chloroquine (Fig. 10A, arrow). Full-length ErbB2 also appeared to be stabilized under these conditions. Including both the full-length and 135-kDa forms of the protein in the quantification, we found that chloroquine substantially slowed ErbB2 degradation (Fig. 8B). Thus, consistent with earlier results (Lerdrup et al., 2006; Tikhomirov and Carpenter, 2000), at least a major fraction of ErbB2 is degraded in lysosomes.

Accumulation of ErbB2 in vesicles containing constitutively active Arf6-Q67L occurred only in the absence of GA

A non-clathrin-mediated endocytic pathway that is regulated by Arf6 has been described (Naslavsky et al., 2003; Naslavsky et al., 2004). Constitutively active Arf6-Q67L causes cargo of this pathway to accumulate in Arf6-Q67L-positive endosomes, which often become enlarged. To determine whether ErbB2 followed this pathway, we expressed HA-tagged Arf6-Q67L in SK-BR-3 cells, treated the cells with GA, and visualized Arf6-Q67L and ErbB2 localization. ErbB2 did not accumulate in Arf6-Q67L-positive endosomes (Fig. 11A). Instead, ErbB2 partially colocalized with GFP-Rab5 and GFP-Rab7, showing that it reached early and late endosomes even in the presence of Arf6-Q67L (Fig. 11B,C). By contrast, ErbB2 accumulated in enlarged Arf6-Q67L-positive endosomes, rather than Rab5- or Rab7-positive endosomes, when cells were not treated with GA (Fig. 11D-F).

We wanted to determine whether Arf6-Q67L affected the degradation of ErbB2. However, the transfection efficiency of SK-BR-3 cells was too low for this. An alternate approach was to express ErbB2 in COS-7 cells, either alone or together with Arf6-Q67L. COS-7 cells express some endogenous ErbB2, which was detectable in our hands by western blotting but not by immunofluorescence microscopy. Western blotting showed that transfected ErbB2 was at least 5- to 10-times more abundant than endogenous ErbB2. Furthermore, immunofluorescence-microscopy analysis showed that at least 80% of cells in co-transfected dishes that expressed

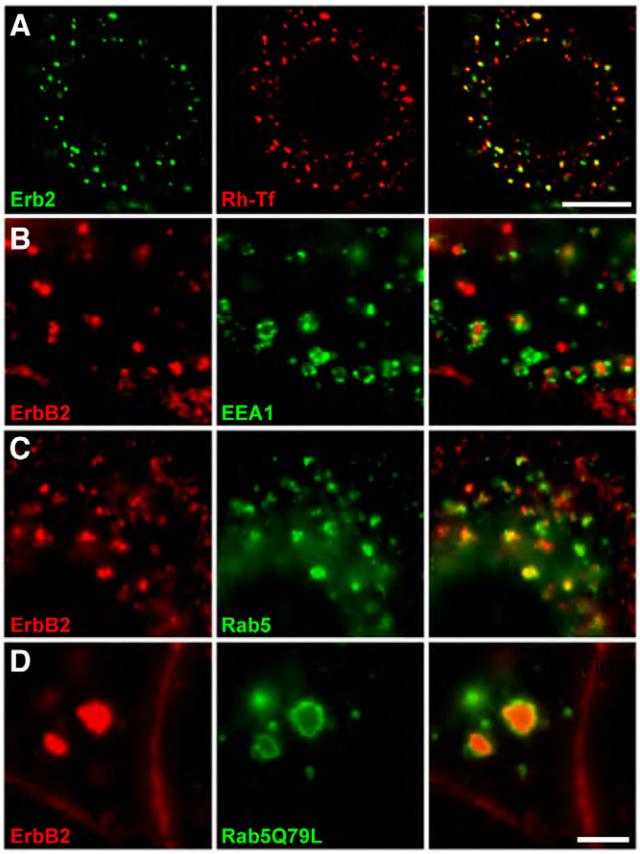

Fig. 8. ErbB2 is delivered to early endosomes after GA treatment. (A-D) SK-BR-3 cells were left untransfected (A,B), or were transiently transfected with GFP-Rab5 (C) or GFP–Rab5-Q79L (D), and then treated with GA for 2 hours (with Rh-Tf added for the last 30 minutes in A), fixed and permeabilized. Left panels: ErbB2, detected with polyclonal antibodies. Center panels: (A) Rh-Tf fluorescence; (B) endogenous EEA1; (C,D) GFP fluorescence. Right panels: merged images. (A) Deconvolved image from a *z*-stack; (B-D) epifluorescence images. Scale bars: 10 μm (A); 5 μm (D, applies to B-D).

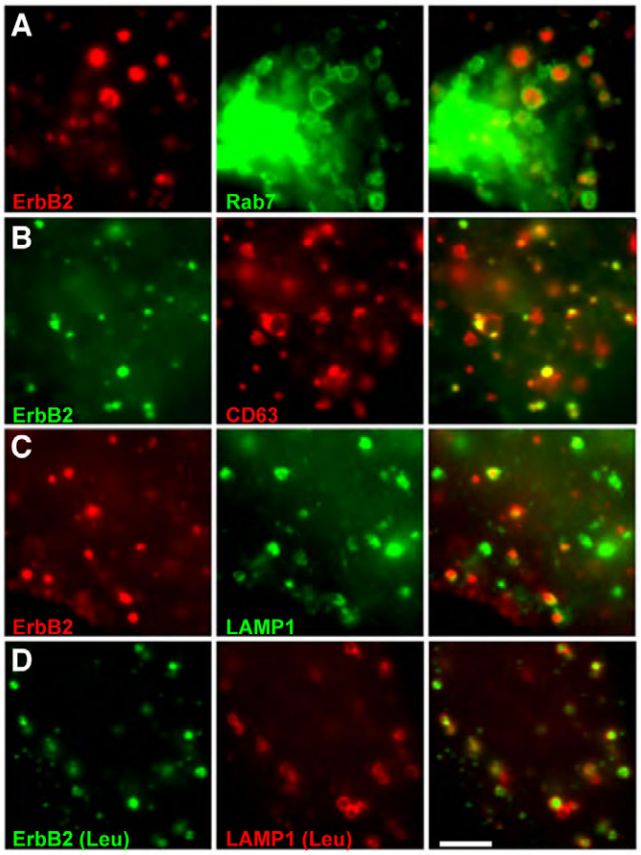

Fig. 9. ErbB2 is delivered to late endosomes and lysosomes after GA treatment. After transient expression of GFP-Rab7 (A only), SK-BR-3 cells were treated with GA for 5 hours (together with 0.1 mg/ml leupeptin, D only), fixed and permeabilized. Left panels: ErbB2 was detected with polyclonal (A,B) or monoclonal (C,D) antibodies and appropriate secondary antibodies. Middle panels: (A) Rab7 (GFP fluorescence); (B) endogenous CD63; (C,D) endogenous LAMP1. Right panels: merged images. Epifluorescence images are shown. Scale bar: 5 μm.

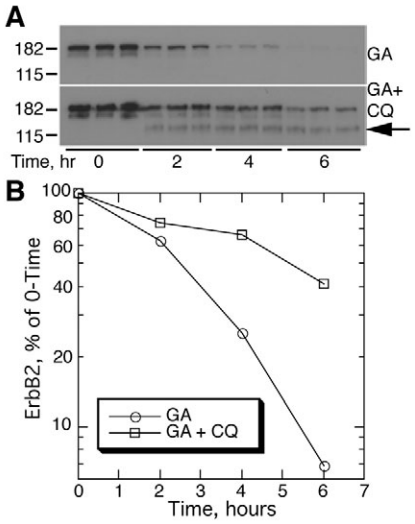

Fig. 10. GA-induced ErbB2 degradation is sensitive to chloroquine. SK-BR-3 cells were incubated with GA with or without chloroquine (CQ) for the times indicated and lysed. Proteins were separated by SDS-PAGE and transferred to membranes for western blotting and detection of ErbB2. (A) Western blots. Top, GA alone; bottom, GA and CQ. Arrow: ca. 135-kDa ErbB2 fragment. (B) Bands were quantified by scanning densitometry and plotted as the percentage of the signal at time=0 remaining at each time point.

ErbB2 also expressed Arf6-Q67L. Thus, this system was feasible for determining the effect of Arf6-Q67L on ErbB2 degradation.

Before doing this, we characterized ErbB2 internalization and trafficking in transfected GA-treated COS-7 cells (supplementary material Fig. S5). After 2 minutes of internalization, most ErbB2 did not colocalize with newly internalized Alexa-Fluor-594-conjugated Tf (supplementary material Fig. S5A, top). Instead, ErbB2 colocalized well with internalized Alexa-Fluor-594-CtxB, -Thy1 and -dextran at this time (supplementary material Fig. S5A, bottom three rows). Dominant-negative dynamin inhibited the internalization of Alexa-Fluor-594-Tf but not ErbB2 (supplementary material Fig. S5B). After prolonged GA treatment, ErbB2 colocalized with early and late endosome markers (supplementary material Fig. S5C). We conclude that ErbB2 followed similar endocytic pathways in COS-7 and SK-BR-3 cells after GA treatment.

Arf6-Q67L did not affect ErbB2 degradation in GA-treated co-transfected COS-7 cells (Fig. 11G,H). Together, these results suggest that, following ErbB2 internalization, Arf6-Q67L inhibited recycling (the normal fate of the protein in the absence of GA), but did not affect degradative transport of ubiquitylated ErbB2 through early and late endosomes to lysosomes in GA-treated cells.

Discussion

GA treatment does not affect ErbB2 internalization

Austin et al. reported that ErbB2 is internalized constitutively, at the same rate with and without GA treatment, and that GA affects ErbB2 trafficking only in endosomes (Austin et al., 2004). They found that, in control cells, ErbB2 recycles to the plasma membrane following internalization, whereas GA induces sorting of ErbB2 into vesicles that bud into the interior of MVBs. Our results agree with these findings. By contrast, another group reported that ErbB2 is resistant to internalization (Hommelgaard et al., 2004) and that GA overcomes this resistance to facilitate endocytosis (Lerdrup et al., 2006; Lerdrup et al., 2007).

The discrepancy between these results might stem from methodological differences. van Deurs and colleagues examined cells by immunofluorescence microscopy after 2-4 hours of GA treatment (Hommelgaard et al., 2004; Lerdrup et al., 2006; Lerdrup et al., 2007). Because they saw internal ErbB2-positive punctae in these cells, but not in control cells, they concluded that ErbB2 underwent endocytosis only after GA treatment. However, by examining cells after short internalization times, Austin et al. showed that ErbB2 is endocytosed constitutively (Austin et al., 2004). Nevertheless, because recycling to the surface is efficient, little internalized ErbB2 is seen at steady state. Examining endocytosis at early times might be especially important for proteins such as ErbB2, which might be internalized more slowly than cargo of the clathrin pathway (Fig. 2A,E). The balance between internalization and recycling might be tilted more heavily in favor of recycling for ErbB2 than for TfR, making it difficult to see internalized protein at steady state.

ErbB2 is internalized by a clathrin-independent pathway

In contrast to our findings, Austin et al. reported that several clathrin-pathway inhibitors affected ErbB2 uptake (Austin et al., 2005). We do not know the explanation for this difference. Austin et al. assayed for inhibition of internalization by binding labeled anti-ErbB2 antibodies to cells, warming for 3 hours with or without inhibitors and then quantifying internalized antibodies. The effects seen after this prolonged internalization time might have resulted from inhibition of recycling, rather than of initial internalization. In fact, prolonged CPZ treatment caused the accumulation of both Tf and ErbB2 in enlarged endosomes, suggesting that recycling was inhibited (D.J.B., unpublished).

Why is EGFR but not ErbB2 targeted to clathrin-coated pits?

Because EGFR and ErbB2 are very similar, it might seem surprising that ErbB2 is not targeted to clathrin-coated pits. Recent findings on the trafficking of EGFR and other ErbB family members can help explain this finding.

EGFR internalization does not require the clathrin adaptor AP2 (Hinrichsen et al., 2003; Motley et al., 2003), but requires Grb2 (Jiang et al., 2003; Wang and Moran, 1996) and c-Cbl or Cbl-b (Ettenberg et al., 1999; Levkowitz et al., 1999). c-Cbl binds tyrosine-phosphorylated EGFR both directly, through its SH2 domain (Galisteo et al., 1995; Levkowitz et al., 1999), and indirectly, via Grb2 (Fukazawa et al., 1996; Jiang et al., 2003; Meisner and Czech, 1995), and ubiquitylates EGFR.

Whereas c-Cbl binds only to tyrosine-phosphorylated EGFR, internalization of ErbB2 in GA-treated cells does not require tyrosine phosphorylation. Furthermore, ErbB family members other than EGFR do not recruit c-Cbl even when activated (Levkowitz et al., 1996; Muthuswamy et al., 1999). Even activated EGFR-ErbB2 heterodimers fail to bind c-Cbl, probably because ErbB2 is unable to phosphorylate the c-Cbl binding site on EGFR (Muthuswamy et al., 1999). This could explain why EGFR is the only ErbB family member that is rapidly downregulated upon activation (King et al., 1988; Lenferink et al., 1998; Stern et al., 1986; Waterman et al., 1998), and why the cytoplasmic domains of ErbB2-4 are internalization-impaired (Baulida et al., 1996; Sorkin et al., 1993; Waterman et al., 1999). As expected, heterodimerization with ErbB2 inhibits EGFR downregulation following ligand binding (Haslekås et al., 2005; Lenferink et al., 1998; Lidke et al., 2004; Muthuswamy et al., 1999; Wang et al., 1999).

It is not clear how c-Cbl stimulates EGFR internalization. According to one model, ubiquitylated EGFR is recognized by

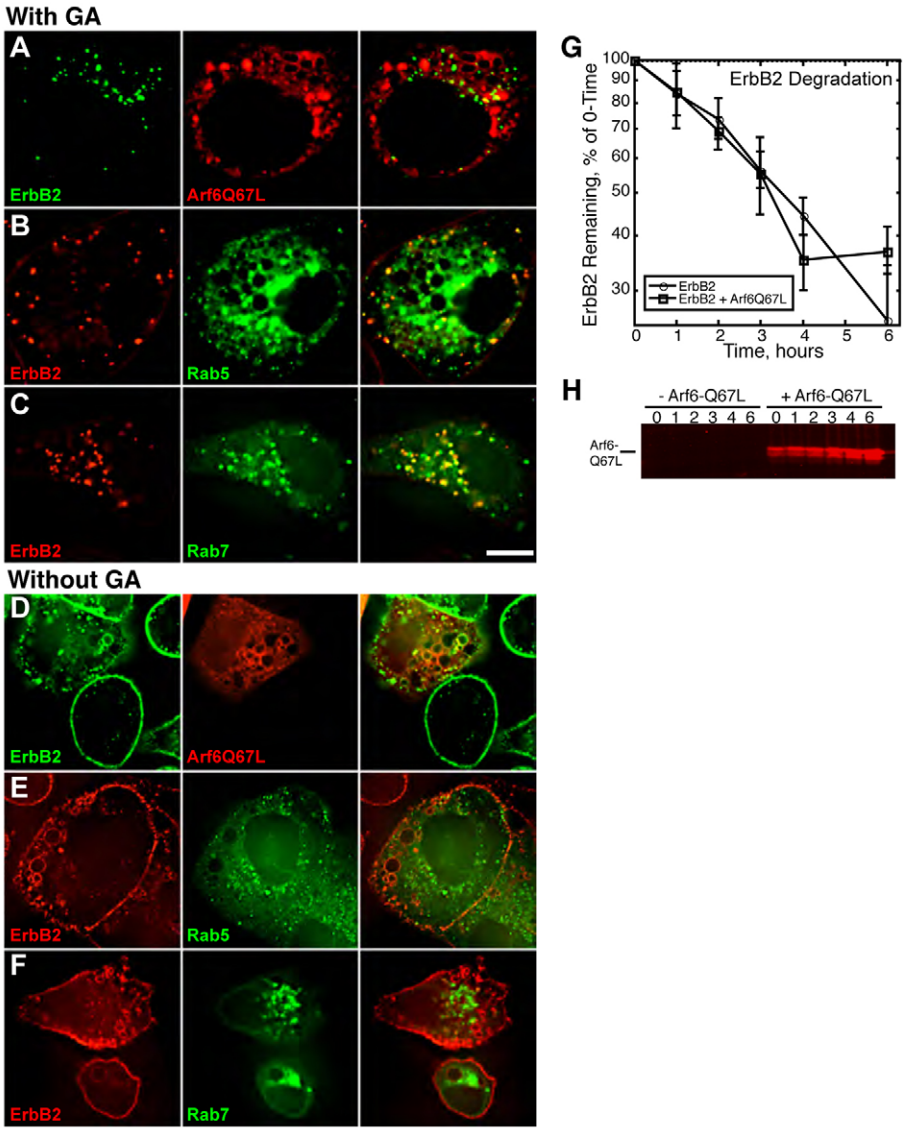

Fig. 11. Accumulation of ErbB2 in Arf-Q67L-positive endosomes occurs only without GA. (A-F) SK-BR-3 cells were transfected with Arf6-Q67L alone (A,D) or in combination with either GFP-Rab5 (B,E) or GFP-Rab7 (C,F). Fl-anti-ErbB2 (A,D) or unlabeled anti-ErbB2 (B,C,E,F) antibodies were bound for 1 hour before cells were warmed for 2 hours with (A-C) or without (D-F) GA. Internalized anti-ErbB2 was detected in fixed and permeabilized cells by Fl-anti-ErbB2 fluorescence (A,D) or with Texas-Red goat-anti-mouse antibodies (B,C,E,F). Although Arf6-Q67L was not visualized in B,C,E or F, vacuoles characteristic of Arf6-Q67L expression were seen. Scale bar: 10 μm. (G,H) COS-7 cells were transfected with ErbB2 alone or together with Arf6-Q67L as indicated. Cells were incubated with GA for the indicated times and solubilized in gel loading buffer. Proteins were separated by SDS-PAGE and transferred to nitrocellulose. ErbB2 and Arf6-Q67L were detected by immunoblotting as described in the Materials and Methods. (H) A representative Arf6-Q67L blot is shown, demonstrating expression in co-transfected cells (+Arf6-Q67L), but not in cells expressing ErbB2 alone (–Arf6-Q67L).

ubiquitin-binding domains of proteins associated with the clathrin coat (de Melker et al., 2004; Fallon et al., 2006; Haglund et al., 2003; Stang et al., 2004). Alternatively, ubiquitylation might target EGFR for clathrin-independent internalization (Sigismund et al., 2005). By contrast, other workers have proposed that ubiquitylation is not required for EGFR internalization (Duan et al., 2003) and that the essential role of c-Cbl in EGFR internalization is independent of ubiquitylation (Huang et al., 2006; Jiang and Sorkin, 2003; Soubeyran et al., 2002). In fact, EGFR Lys mutants, which show 70-80% reduced ligand-stimulated ubiquitylation, are internalized normally (Huang et al., 2006). A ubiquitin-independent role of c-Cbl in EGFR internalization would probably involve a complex of c-Cbl, CIN85 and endophilin; this complex has been reported to be required for EGFR endocytosis (Soubeyran et al., 2002). In any case, an essential role for c-Cbl in efficient EGFR internalization seems clear. The failure of ErbB2 to bind c-Cbl could explain why it is not targeted to clathrin-coated pits.

If ubiquitylation signals for EGFR internalization, then ubiquitylation of ErbB2 by CHIP could play a similar role, possibly targeting ErbB2 for clathrin-independent internalization, as reported for EGFR (Sigismund et al., 2005). However, in contrast to that report, we found that ErbB2 internalization did not occur via caveolae in SK-BR-3 cells. Furthermore, the finding that GA did not affect the internalization rate of ErbB2 argues against a role for ubiquitylation in internalization.

Relation of ErbB2 endocytosis to other non-clathrin pathways

ErbB2 internalization in SK-BR-3 cells did not occur via caveolae, because these cells lack caveolae (Hommelgaard et al., 2004). Furthermore, unlike caveolar endocytosis (Henley et al., 1998) and also unlike a pathway used to internalize the interleukin-2 receptor in lymphocytes (Lamaze et al., 2001), ErbB2 internalization did not require dynamin. ErbB2 internalization differed from a ‘caveolar-like’ pathway that operates in cells lacking caveolae (Damm et al., 2005) in that it did not require tyrosine-kinase activity.

ErbB2 internalization was similar to the GEEC and/or CLIC pathways (Kalia et al., 2006; Kirkham et al., 2005; Sabharanjak et al., 2002) in that it did not require clathrin, dynamin or caveolae. In addition, newly internalized ErbB2 colocalized with GPI-anchored proteins, CtxB and a fluid-phase marker. Structures

containing newly internalized ErbB2 often had the distinctive appearance of CLICs. Nevertheless, in SK-BR-3 cells, internalization of ErbB2 and a fluid-phase marker did not require Rho-family GTPase activity. Independence of Rho-family GTPases in this GEEC-like pathway might reflect cell-type differences, possibly including the transformed state of SK-BR-3 cells.

ErbB2 accumulated in Arf6-Q67L-positive endosomes in control cells, which is in common with cargo of the Arf6-regulated pathway. However, after GA treatment, ErbB2 was transported normally to lysosomes for degradation. Arf6-Q67L might prevent internalized ErbB2 from recycling, causing it to accumulate in swollen vacuoles in the absence of GA, but not inhibit ubiquitin-based sorting into MVBs and downstream transport to lysosomes. Our finding contrasts with an earlier report that indicated that Arf6-Q67L inhibited transport of MHC class I protein and CD59 to lysosomes for degradation (Naslavsky et al., 2004). The difference might result from the fact that ErbB2, unlike the markers examined in the earlier study, was ubiquitylated.

How ErbB2 might be targeted for internalization

We do not know what targets ErbB2 for internalization by the pathway we have described. A clue might come from the characteristics of the GEEC and/or CLIC pathway(s) (Kalia et al., 2006; Kirkham et al., 2005; Sabharanjak et al., 2002). Both GPI-anchored proteins and CtxB have a high affinity for lipid rafts, or membrane microdomains in the liquid-ordered phase. ErbB2 can be enriched in detergent-resistant membranes, an indication of high raft affinity (Hommelgaard et al., 2004; Nagy et al., 2002; Yang et al., 2004; Zhou and Carpenter, 2001; Zurita et al., 2004). Thus, a subset of transmembrane proteins with high raft affinity might be targeted to the GEEC and/or CLIC pathways, and to the GEEC-like pathway that is followed by ErbB2 in SK-BR-3 cells.

Downstream trafficking of ErbB2

As reported previously (Austin et al., 2004), ErbB2 was transported to EEA1-positive early endosomes after internalization. These workers also found ErbB2 in vesicles inside MVBs in GA-treated cells, suggesting transport to degradative compartments (Austin et al., 2004). However, they noted that ErbB2-positive MVBs retained immature characteristics, such as recycling tubules, even after prolonged GA treatment. They were also surprised to see poor colocalization of ErbB2 with the late-endosome marker CD63 (Austin et al., 2004). By contrast, we saw good colocalization of ErbB2 with CD63 and LAMP1, especially after treatment with leupeptin or chloroquine. ErbB2 degradation was inhibited by chloroquine when blots were probed with extracellular-domain-specific antibodies, confirming previous work (Tikhomirov and Carpenter, 2000; Tikhomirov and Carpenter, 2001) and suggesting that the apparent chloroquine insensitivity reported initially (Citri et al., 2002; Mimnaugh et al., 1996; Way et al., 2004) resulted from the inability of blotting antibodies to detect a clipped form of the protein.

In summary, we showed that, after GA treatment, ErbB2 is internalized by a non-clathrin, non-caveolar pathway, and then merges with the classical endocytic pathway for transport to lysosomes and degradation.

Materials and Methods

Cells and transfection

SK-BR-3 human breast cancer cells and COS-7 cells were maintained in Dulbecco's modified Eagle's medium with 10% iron-supplemented calf serum (JRH Biosciences) and penicillin/streptomycin. Cells were transiently transfected with Lipofectamine 2000 (Invitrogen) and examined 1-2 days post-transfection, except for cells expressing Arf6-Q67L, which were examined at 14-16 hours post-transfection.

Plasmids

GFP-Eps15 mutant ΔE95/295 (Benmerah et al., 1999) was from Alexandre Benmerah (Institut Cochin, Paris, France). Tetracycline-inducible dominant-negative (K44A) HA-dynamin-1 (Damke et al., 1994), co-expressed with pTet-Off (Clontech), was from Jeffrey Pessin (Albert Einstein University, Bronx, NY). HA-Arf6-Q67L (Hernández-Deviez et al., 2004) in pCB7 (Frank et al., 1998) was from James Casanova (University of Virginia, Charlottesville, VA). pBC12/PLAP was described previously (Berger et al., 1987). EGFP-bound wild-type and mutant (Q79L) Rab5 (Volpicelli et al., 2001) were from Allan Levey (Emory University, Atlanta GA). GFP Rab7 (Guignot et al., 2004) was from Craig Roy (Yale University, New Haven, CT). 3×HA-tagged wild-type and dominant-negative forms of RhoA and Cdc42 (containing T19N and T17N mutations, respectively) were from University of Missouri-Rolla cDNA Resource Center (www.cDNA.org). Mouse Thy1.1 (Zhang et al., 1991) was from John Rose (Yale University, New Haven, CT). pEGFP-2×FYVE (Petiot et al., 2003) was from William Maltese (University of Toledo, Toledo, OH). Human ErbB2 in pcDNA3 was from Len Neckers (NIH).

Antibodies, fluorescent compounds and other reagents

Anti-ErbB2 antibodies: for immunofluorescence microscopy, monoclonal antibodies 4D5 [purified from supernatant of hybridoma cells (ATCC) grown in an Integra Biosciences CELLine two-compartment bioreactor, from Microbiology International (Frederick, MD)], or 9G6.10 or N28 (for acid-stripping experiments) from LabVision were used for cell-surface detection. Rabbit polyclonal anti-ErbB2 antibodies (DakoCytomation USA) or monoclonal antibodies l were used on fixed, permeabilized cells. LabVision anti-ErbB2 antibody #20 was used on blots.

Other mouse monoclonal antibodies: anti-HA tag from Applied Biological Materials; anti-phosphotyrosine from Upstate Biological; anti-EGFR #3 from LabVision; anti-EEA1 and anti-Thy1 (OX-7) from BD Biosciences; and anti-CD63 from the Developmental Studies Hybridoma Bank, University of Iowa.

Rabbit polyclonal antibodies: anti-clathrin heavy chain (Simpson et al., 1996) from Margaret S. Robinson (University of Cambridge, Cambridge, UK); anti-HA tag from Santa Cruz Biotechnology; anti-LAMP-1 from Affinity Bioreagents; and anti-PLAP from DakoCytomation USA. Anti-PLAP Fab fragments were prepared using immobilized papain and anti-Thy-1.1 Fab fragments using immobilized ficin (Pierce) using the suppliers' instructions. Cleavage was verified by western blotting. Fluorescein was conjugated to anti-ErbB2 and anti-EGFR antibodies, and to anti-PLAP Fab fragments; rhodamine to human Tf; Alexa-Fluor-594 to anti-Thy1 Fab fragments; and biotin to anti-ErbB2 antibodies, Tf and bovine serum albumin (BSA) by using N-hydroxysuccinimide-linked fluorescein, rhodamine Alexa-Fluor-594 or PEO_4-biotin (Pierce), using conditions recommended by the supplier. Dichlorotriazinylaminofluorescein-goat anti-mouse IgG, fluorescein-goat anti-rabbit IgG, Texas-Red-goat anti-mouse IgG, Texas-Red-goat anti-rabbit IgG and horseradish-peroxidase-goat anti-mouse IgG were from Jackson ImmunoResearch Laboratories. Alexa-Fluor-350-goat anti-mouse and anti-rabbit IgGs, Alexa-Fluor-594-CtxB, and Alexa-Fluor-680 goat anti-mouse IgG and Alexa-Fluor-680 goat anti-rabbit IgG were used for fluorescent detection of bands on blots. FluoroRuby dextran (10,000 MW), Alexa-Fluor-594-Tf and rhodamine-phalloidin were from Molecular Probes, Invitrogen. Where indicated, the Alexa-Fluor-488 Zenon Mouse IgG labeling kit (Invitrogen), consisting of fluorescently tagged Fab fragments of goat antibodies directed against the Fc portion of mouse IgG, was used to detect anti-ErbB2 antibodies. Other reagents: GA (used at 5 μM) was from the Drug Synthesis and Chemistry Branch, National Cancer Institute (Bethesda, MD); EGF from EMD Biosciences; Clostridium difficile toxin B from Tech Lab; LY294002 from Cayman Chemicals; and peroxidase-conjugated streptavidin polymer from Sigma Aldrich or Fitzgerald Industries. Other reagents were from Sigma Aldrich.

Fluorescence microscopy

Fluorescence microscopy was as described previously (Ostermeyer et al., 2004) except that, for detection of LAMP-1, fixed cells were permeabilized with phosphate-buffered saline (PBS) containing 0.5% saponin and then treated for 10 minutes at room temperature with PBS (150 mM NaCl, 20 mM phosphate buffer, pH 7.4) containing 0.1% sodium borohydride and 0.1% saponin. 0.1% saponin was included in all further incubations.

For internalization assays, antibodies (2 μg/ml) were bound to cells at 4°C for 1 hour before starting internalization by the addition of pre-warmed media. Residual surface-bound antibodies were stripped with acid (100 mM Gly, 50 mM KCl, 20 mM magnesium acetate, pH 2.3), using three washes of 3 minutes each. Fluorescent Tf (35 μg/ml) was either bound to cells with antibodies or included in the media during warming, as indicated.

Images shown were captured and processed by epifluorescence microscopy as described (Ostermeyer et al., 2001; Ostermeyer et al., 2004), or by deconvolution microscopy using a Zeiss Axiovert 200 deconvolution microscope and processing with Axiovision software (version 4.4). To acquire *z*-stacks, 25-35 serial images were recorded at 350-nm intervals along the *z*-axis using a 63× or 100× oil-immersion objective. Out-of-plane fluorescence was removed by deconvolution using the

inverse filter algorithm or a modification of the constrained iterative algorithm. Images shown are representative sections from deconvolved *z*-stacks or maximum intensity projections of *z*-stacks.

Colocalization analysis was performed on images obtained with a Zeiss LSM 5 Pascal confocal laser-scanning microscope using ImageJ (http://rsb.info.nih.gov/ij) and the JaCoP plug-in (Bolte and Cordelières, 2006). Manders coefficients M1 and M2, reflecting channel1-channel2 overlap and channel2-channel1 overlap, respectively, are shown in Figs 2H and 5E. Pilot experiments were performed to determine effective maximum and minimum colocalization values. Maximal M1 and M2 values (colocalization of internalized Fl-anti-ErbB2 and Texas-Red-goat anti-mouse secondary antibodies) ranged from 0.7 to 0.8. Minimal values (colocalization of early endosomes, visualized with Alexa-Fluor-594-Tf internalized for 10 minutes, and the Golgi, visualized with anti-GM130 and dichlorotriazinylaminofluorescein-goat anti-mouse IgG) ranged from 0.05 to 0.20.

CELISA to measure ErbB2, Tf or BSA internalization

SK-BR-3 cells seeded in 35-mm dishes the day before the assay (3×10^5 cells/dish) were pretreated with GA and/or other drugs for 45 minutes, except as noted. Biotinylated anti-ErbB2 antibodies (15 μg/ml) were bound for 2 hours at 4°C. After washing with Hanks' balanced salt solution (Invitrogen), prewarmed media was added for various times. Internalization was stopped by washing with ice-cold Hanks' balanced salt solution and transferring dishes to ice. To mask residual surface-bound antibodies, cells were incubated with streptavidin (40 μg/ml) for 1 hour at 4°C. After washing, cells were paraformaldehyde-fixed, permeabilized and blocked as for immunofluorescence microscopy. Cells were then incubated with peroxidase-conjugated streptavidin polymer (1 μg/ml in PBS with 0.05% Tween 20) for 1 hour at room temperature. After washing, SureBlue Reserve tetramethylbenzidine (TMB) substrate (KPL, Gaithersburg, MD) was added for 10 seconds, before stopping the reaction with TMB stop solution and measuring absorbance (450 nm) in a spectrophotometer. Except as noted, background (signal in control dishes left on ice) was subtracted from all values. Assays for biotinylated Tf (75 μg/ml) or BSA (5 mg/ml) uptake were the same, except they were not pre-bound, but added to media for internalization. Tenfold excess unlabeled Tf reduced biotinylated-Tf signal to background after a 20-minute uptake (A.G.O.-F., unpublished).

Other methods

Sodium dodecyl sulfate polyacrylamide gel electrophoresis (SDS-PAGE), transfer to polyvinylidene difluoride, western blotting and detection by enhanced chemiluminescence were as described (Arreaza et al., 1994). Bands were scanned and quantified using NIH Image. For Fig. 11G,H, blots were incubated with Alexa-Fluor-680-conjugated secondary antibodies, and detected and quantified with the Odyssey-Infrared Imaging System (LI-COR Biosciences).

We thank Alexandre Benmerah, James Casanova, Allan Levey, William Maltese, Len Neckers, Jeffrey Pessin, John Rose and Craig Roy for plasmids; Margaret S. Robinson for anti-clathrin antibodies; and Robert Haltiwanger and Laura Listenberger for reading the manuscript. This work was supported by grant GM47897 (to D.A.B.) from the National Institutes of Health.

References

Arreaza, G., Melkonian, K. A., LaFevre-Bernt, M. and Brown, D. A. (1994). Triton X-100-resistant membrane complexes from cultured kidney epithelial cells contain the Src-family protein tyrosine kinase p62^{yes}. *J. Biol. Chem.* **269**, 19123-19127.

Austin, C. D., De Mazière, A. M., Pisacane, P. I., van Dijk, S. M., Eigenbrot, C., Sliwkowski, M. X., Klumperman, J. and Scheller, R. H. (2004). Endocytosis and sorting of ErbB2 and the site of action of cancer therapeutics trastuzumab and geldanamycin. *Mol. Biol. Cell* **15**, 5268-5282.

Austin, C. D., Wen, X., Gazzard, L., Nelson, C., Scheller, R. H. and Scales, S. J. (2005). Oxidizing potential of endosomes and lysosomes limits intracellular cleavage of disulfide-based antibody-drug conjugates. *Proc. Natl. Acad. Sci. USA* **102**, 17987-17992.

Baulida, J., Kraus, M. H., Alimandi, M., DiFiore, P. P. and Carpenter, G. (1996). All ErbB receptors other than the epidermal growth factor receptor are endocytosis impaired. *J. Biol. Chem.* **271**, 5251-5257.

Beerli, R. R., Graus-Porta, D., Woods-Cook, K., Chen, X., Yarden, Y. and Hynes, N. E. (1995). Neu differentiation factor activation of ErbB-3 and ErbB-4 is cell specific and displays a differential requirement for ErbB-2. *Mol. Cell. Biol.* **15**, 6496-6505.

Benmerah, A., Bayrou, M., Cerf-Bensussan, N. and Dautry-Varsat, A. (1999). Inhibition of clathrin-coated pit assembly by an Eps15 mutant. *J. Cell Sci.* **112**, 1303-1311.

Berger, J., Howard, A. D., Gerber, L., Cullen, B. R. and Udenfriend, S. (1987). Expression of active, membrane-bound human placental alkaline phosphatase by transfected simian cells. *Proc. Natl. Acad. Sci. USA* **84**, 4885-4889.

Bolte, S. and Cordelières, F. P. (2006). A guided tour into subcellular colocalization analysis in light microscopy. *J. Microsc.* **224**, 213-232.

Bryant, D. M., Kerr, M. C., Hammond, L. A., Joseph, S. R., Mostov, K. E., Teasdale, R. D. and Stow, J. L. (2007). EGF induces macropinocytosis and SNX1-modulated recycling of E-cadherin. *J. Cell Sci.* **120**, 1818-1828.

Chadda, R., Howes, M. T., Plowman, S. J., Hancock, J. F., Parton, R. G. and Mayor, S. (2007). Cholesterol-sensitive Cdc42 activation regulates actin polymerization for endocytosis via the GEEC pathway. *Traffic* **8**, 702-717.

Cheng, Z. J., Singh, R. D., Sharma, D. K., Holicky, E. L., Hanada, K., Marks, D. L. and Pagano, R. E. (2006). Distinct mechanisms of clathrin-independent endocytosis have unique sphingolipid requirements. *Mol. Biol. Cell* **17**, 3197-3210.

Citri, A., Alroy, I., Lavi, S., Rubin, C., Xu, W., Grammatikakis, N., Patterson, C., Neckers, L., Fry, D. W. and Yarden, Y. (2002). Drug-induced ubiquitylation and degradation of ErbB receptor tyrosine kinases: implications for cancer therapy. *EMBO J.* **21**, 2407-2417.

Citri, A., Kochupurakkal, B. S. and Yarden, Y. (2004). The Achilles heel of ErbB-2/HER2: regulation by the Hsp90 chaperone machine and potential for pharmacological intervention. *Cell Cycle* **3**, 51-60.

Conner, S. D. and Schmid, S. L. (2003). Regulated portals of entry into the cell. *Nature* **422**, 37-44.

Damke, H., Baba, T., Warnock, D. E. and Schmid, S. L. (1994). Induction of mutant dynamin specifically blocks endocytic coated vesicle formation. *J. Cell Biol.* **127**, 915-934.

Damm, E.-M., Pelkmans, L., Kartenbeck, J., Mezzacasa, A., Kurzchalia, T. and Helenius, A. (2005). Clathrin- and caveolin-1-independent endocytosis: entry of simian virus 40 into cells devoid of caveolae. *J. Cell Biol.* **168**, 477-488.

de Melker, A. A., van der Horst, G. and Borst, J. (2004). Ubiquitin ligase activity of c-Cbl guides the epidermal growth factor receptor into clathrin-coated pits by two distinct modes of Eps15 recruitment. *J. Biol. Chem.* **279**, 55465-55473.

Duan, L., Miura, Y., Dimri, M., Majumder, B., Dodge, I. L., Reddi, A. L., Ghosh, A., Fernandes, N., Zhou, P., Mullane-Robinson, K. et al. (2003). Cbl-mediated ubiquitinylation is required for lysosomal sorting of epidermal growth factor receptor but is dispensable for endocytosis. *J. Biol. Chem.* **278**, 28950-28960.

Ettenberg, S. A., Keane, M. M., Nau, M. M., Frankel, M., Wang, L. M., Pierce, J. H. and Lipkowitz, S. (1999). cbl-b inhibits epidermal growth factor receptor signaling. *Oncogene* **18**, 1855-1866.

Fallon, L., Bélanger, C. M. L., Corera, A. T., Kontogiannea, M., Regan-Klapisz, E., Moreau, F., Voortman, J., Haber, M., Rouleau, G., Thorarinsdottir, T. et al. (2006). A regulated interaction with the UIM protein Eps15 implicates parkin in EGF receptor trafficking and PI(3)K-Akt signalling. *Nat. Cell Biol.* **8**, 834-842.

Frank, S. R., Hatfield, J. C. and Casanova, J. E. (1998). Remodeling of the actin cytoskeleton is coordinately regulated by protein kinase C and the ADP-ribosylation factor nucleotide exchange factor ARNO. *Mol. Biol. Cell* **9**, 3133-3146.

Fukazawa, T., Miyake, S., Band, V. and Band, H. (1996). Tyrosine phosphorylation of Cbl upon epidermal growth factor (EGF) stimulation and its association with EGF receptor and downstream signaling proteins. *J. Biol. Chem.* **271**, 14554-14559.

Galisteo, M. L., Dikic, I., Batzer, A. G., Langdon, W. Y. and Schlessinger, J. (1995). Tyrosine phosphorylation of the c-cbl proto-oncogene protein product and association with epidermal growth factor (EGF) receptor upon EGF stimulation. *J. Biol. Chem.* **270**, 20242-20245.

Garrett, W. S., Chen, L.-M., Kroschewski, R., Ebersold, M., Turley, S., Trombetta, S., Galán, J. E. and Mellman, I. (2000). Developmental control of endocytosis in dendritic cells by cdc42. *Cell* **102**, 325-334.

Graus-Porta, D., Beerli, R. R., Daly, J. M. and Hynes, N. E. (1997). ErbB-2, the preferred heterodimerization partner of all ErbB receptors, is a mediator of lateral signaling. *EMBO J.* **16**, 1647-1655.

Gu, F. and Gruenberg, J. (2000). ARF1 regulates pH-dependent COP functions in the early endocytic pathway. *J. Biol. Chem.* **275**, 8154-8160.

Guignot, J., Caron, E., Beuzon, C., Bucci, C., Kagan, J., Roy, C. and Holden, D. W. (2004). Microtubule motors control membrane dynamics of Salmonella-containing vacuoles. *J. Cell Sci.* **117**, 1033-1045.

Haglund, K., Sigismund, S., Polo, S., Szymkiewicz, I., Di Fiore, P. P. and Dikic, I. (2003). Multiple monoubiquitination of RTKs is sufficient for their endocytosis and degradation. *Nat. Cell Biol.* **5**, 461-466.

Haslekås, C., Breen, K., Pedersen, K. W., Johannessen, L. E., Stang, E. and Madshus, I. H. (2005). The inhibitory effect of ErbB2 on epidermal growth factor-induced formation of clathrin-coated pits correlates with retention of epidermal growth factor receptor-ErbB2 oligomeric complexes at the plasma membrane. *Mol. Biol. Cell* **16**, 5832-5842.

Henley, J. R., Kruegger, E. W. A., Oswald, B. J. and McNiven, M. A. (1998). Dynamin-mediated internalization of caveolae. *J. Cell Biol.* **141**, 85-99.

Hernández-Deviez, D. J., Roth, M. G., Casanova, J. E. and Wilson, J. M. (2004). ARNO and ARF6 regulate axonal elongation and branching through downstream activation of phosphatidylinositol 4-phosphate 5-kinase alpha. *Mol. Biol. Cell* **15**, 111-120.

Hinrichsen, L., Harborth, J., Andrees, L., Weber, K. and Ungewickell, E. J. (2003). Effect of clathrin heavy chain- and alpha-adaptin-specific small inhibitory RNAs on endocytic accessory proteins and receptor trafficking in HeLa cells. *J. Biol. Chem.* **278**, 45160-45170.

Hohfeld, J., Cyr, D. M. and Patterson, C. (2001). From the cradle to the grave: molecular chaperones that may choose between folding and degradation. *EMBO Rep.* **2**, 885-890.

Hommelgaard, A. M., Lerdrup, M. and van Deurs, B. (2004). Association with membrane protrusions makes ErbB2 an internalization-resistant receptor. *Mol. Biol. Cell* **15**, 1557-1567.

Huang, F., Kirkpatrick, D., Jiang, X., Gygi, S. and Sorkin, A. (2006). Differential regulation of EGF receptor internalization and degradation by multiubiquitination within the kinase domain. *Mol. Cell* **21**, 737-748.

Jank, T., Giesemann, T. and Astories, K. (2007). Rho-glucosylating Clostridium difficile toxins A and B: new insights into structure and function. *Glycobiology* **17**, 15R-22R.

Jiang, X. and Sorkin, A. (2003). Epidermal growth factor receptor internalization through clathrin-coated pits requires Cbl RING finger and proline-rich domains but not receptor polyubiquitylation. *Traffic* **4**, 529-543.
Jiang, X., Huang, F., Marusyk, A. and Sorkin, A. (2003). Grb2 regulates internalization of EGF receptors through clathrin-coated pits. *Mol. Biol. Cell* **14**, 858-870.
Kalia, M., Kumari, S., Chadda, R., Hill, M. M., Parton, R. G. and Mayor, S. (2006). Arf6-independent GPI-anchored protein-enriched early endosomal compartments fuse with sorting endosomes via a Rab5/phosphatidylinositol-3′-kinase-dependent machinery. *Mol. Biol. Cell* **17**, 3689-3704.
King, C. R., Borrello, I., Bellot, F., Comoglio, P. and Schlessinger, J. (1988). EGF binding to its receptor triggers a rapid tyrosine phosphorylation of the ErbB-2 protein in the mammary tumor cell line SK-BR-3. *EMBO J.* **7**, 1647-1651.
Kirkham, M. and Parton, R. G. (2005). Clathrin-independent endocytosis: new insights into caveolae and non-caveolar lipid raft carriers. *Biochim. Biophys. Acta* **1745**, 273-286.
Kirkham, M., Fujita, A., Chadda, R., Nixon, S. J., Kurzchalia, T. V., Sharma, D. K., Pagano, R. E., Hancock, J. F., Mayor, S. and Parton, R. G. (2005). Ultrastructural identification of uncoated caveolin-independent early endocytic vehicles. *J. Cell Biol.* **168**, 465-476.
Kumari, S. and Mayor, S. (2008). ARF1 is directly involved in dynamin-independent endocytosis. *Nat. Cell Biol.* **10**, 30-41.
Lamaze, C., Dujeancourt, A., Baba, T., Lo, C. G., Benmerah, A. and Dautry-Varsat, A. (2001). Interleukin 2 receptors and detergent-resistant membrane domains define a clathrin-independent endocytic pathway. *Mol. Cell* **7**, 661-671.
Lange, Y. and Steck, T. L. (1984). Mechanism of red blood cell acanthocytosis and echinocytosis in vivo. *J. Membr. Biol.* **77**, 153-159.
Lencer, W. I. and Saslowsky, D. (2005). Raft trafficking of AB(5) subunit bacterial toxins. *Biochim. Biophys. Acta* **1746**, 314-321.
Lenferink, A. E. G., Pinkas-Kramarski, R., van de Poll, M. L. M., van Vugt, M. J. H., Klapper, L. N., Tzahar, E., Waterman, H., Sela, M., van Zoelen, E. J. J. and Yarden, Y. (1998). Differential endocytic routing of homo- and hetero-dimeric ErbB tyrosine kinases confers signaling superiority to receptor heterodimers. *EMBO J.* **17**, 3385-3397.
Lerdrup, M., Hommelgaard, A. M., Grandal, M. and van Deurs, B. (2006). Geldanamycin stimulates internalization of ErbB2 in a proteasome-dependent way. *J. Cell Sci.* **119**, 85-95.
Lerdrup, M., Bruun, S., Grandal, M. V., Roepstorff, K., Kristensen, M. M., Hommelgaard, A. M. and van Deurs, B. (2007). Endocytic down-regulation of ErbB2 is stimulated by cleavage of its C-terminus. *Mol. Biol. Cell* **18**, 3656-3666.
Levkowitz, G., Klapper, L. N., Tzahar, E., Freywald, A., Sela, M. and Yarden, Y. (1996). Coupling of the c-Cbl protooncogene product to Erb-1/EGF-receptor but not to other ErbB proteins. *Oncogene* **12**, 1117-1125.
Levkowitz, G., Waterman, H., Ettenberg, S. A., Katz, M., Tsygankov, A. Y., Alroy, I., Lavi, S., Iwai, K., Reiss, Y., Ciechanover, A. et al. (1999). Ubiquitin ligase activity and tyrosine phosphorylation underlie suppression of growth factor signaling by c-Cbl/Sli-1. *Mol. Cell* **4**, 1029-1040.
Lidke, D. S., Nagy, P., Heintzmann, R., Arndt-Jovin, D. J., Post, J. N., Grecco, H. E., Jares-Erijman, E. A. and Jovin, T. M. (2004). Quantum dot ligands provide new insights into erbB/HER receptor-mediated signal transduction. *Nat. Biotechnol.* **22**, 198-203.
Mayor, S. and Pagano, R. E. (2007). Pathways of clathrin-independent endocytosis. *Nat. Rev. Mol. Cell. Biol.* **8**, 603-612.
Meisner, H. and Czech, M. P. (1995). Coupling of the proto-oncogene product c-Cbl to the epidermal growth factor receptor. *J. Biol. Chem.* **270**, 25332-25335.
Mimnaugh, E. G., Chavany, C. and Neckers, L. (1996). Polyubiquitination and proteasomal degradation of the p185c-ErbB-2 receptor protein-tyrosine kinase induced by geldanamycin. *J. Biol. Chem.* **271**, 22796-22801.
Motley, A., Bright, N. A., Seaman, M. N. J. and Robinson, M. S. (2003). Clathrin-mediated endocytosis in AP-2-depleted cells. *J. Cell Biol.* **162**, 909-918.
Muthuswamy, S. K., Gilman, M. and Brugge, J. S. (1999). Controlled dimerization of ErbB receptors provides evidence for differential signaling by homo- and heterodimers. *Mol. Cell. Biol.* **19**, 6845-6857.
Nagy, P., Vereb, G., Sebestyén, Z., Horváth, G., Lockett, S. J., Damjanovich, S., Park, J. W., Jovin, T. M. and Szöllosi, J. (2002). Lipid rafts and the local density of ErbB proteins influence the biological role of homo- and heteroassociations of ErbB2. *J. Cell Sci.* **115**, 4251-4262.
Naslavsky, N., Weigert, R. and Donaldson, J. G. (2003). Convergence of non-clathrin- and clathrin-derived endosomes involves Arf6 inactivation and changes in phosphoinositides. *Mol. Biol. Cell* **14**, 417-431.
Naslavsky, N., Weigert, R. and Donaldson, J. G. (2004). Characterization of a nonclathrin endocytic pathway: membrane cargo and lipid requirements. *Mol. Biol. Cell* **15**, 3542-3552.
Ostermeyer, A. G., Paci, J. M., Zeng, Y., Lublin, D. M., Munro, S. and Brown, D. A. (2001). Accumulation of caveolin in the endoplasmic reticulum redirects the protein to lipid storage droplets. *J. Cell Biol.* **152**, 1071-1078.
Ostermeyer, A. G., Ramcharan, L. T., Zeng, Y., Lublin, D. M. and Brown, D. A. (2004). Role of the hydrophobic domain in targeting caveolin-1 to lipid droplets. *J. Cell Biol.* **164**, 69-78.
Pellegrin, S. and Mellor, H. (2007). Actin stress fibres. *J. Cell Sci.* **120**, 3491-3499.
Petiot, A., Faure, J., Stenmark, H. and Gruenberg, J. (2003). PI3P signaling regulates receptor sorting but not transport in the endosomal pathway. *J. Cell Biol.* **162**, 971-979.
Richter, K. and Buchner, J. (2001). Hsp90: Chaperoning signal transduction. *J. Cell Physiol.* **188**, 281-290.
Ridley, A. J., Paterson, H. F., Johnston, C. L., Diekmann, D. and Hall, A. (1992). The small GTP-binding protein rac regulates growth factor-induced membrane ruffling. *Cell* **70**, 401-410.
Sabharanjak, S., Sharma, P., Parton, R. G. and Mayor, S. (2002). GPI-anchored proteins are delivered to recycling endosomes via a distinct cdc42-regulated, clathrin-independent pinocytic pathway. *Dev. Cell* **2**, 411-423.
Sandvig, K. and Van Deurs, B. (2002). Transport of protein toxins into cells: pathways used by ricin, cholera toxin and Shiga toxin. *FEBS Lett.* **529**, 49-53.
Schnatwinkel, C., Christoforidis, S., Lindsay, M. R., Uttenweiler-Joseph, S., Wilm, M., Parton, R. G. and Zerial, M. (2004). The Rab5 effector Rabankyrin-5 regulates and coordinates different endocytic mechanisms. *PLoS Biol.* **2**, E261.
Sharma, D. K., Brown, J. C., Choudhury, A., Peterson, T. E., Holicky, E., Marks, D. L., Simari, R., Parton, R. G. and Pagano, R. E. (2004). Selective stimulation of caveolar endocytosis by glycosphingolipids and cholesterol. *Mol. Biol. Cell* **15**, 3114-3122.
Sharp, S. and Workman, P. (2006). Inhibitors of the HSP90 molecular chaperone: Current status. *Adv. Cancer Res.* **95**, 323-348.
Sigismund, S., Woelk, T., Puri, C., Maspero, E., Tacchetti, C., Transidico, P., Di Fiore, P. P. and Polo, S. (2005). Clathrin-independent endocytosis of ubiquitinated cargos. *Proc. Natl. Acad. Sci. USA* **102**, 2760-2765.
Simpson, F., Bright, N. A., West, M. A., Newman, L. S., Darnell, R. B. and Robinson, M. S. (1996). A novel adaptor-related protein complex. *J. Cell Biol.* **133**, 749-760.
Slamon, D. J., Clark, G. M., Wong, S. G., Levin, W. J., Ullrich, A. and McGuire, W. L. (1987). Human breast cancer: correlation of relapse and survival with amplification of the HER-2/neu oncogene. *Science* **235**, 177-182.
Sorkin, A., DiFiore, P. P. and Carpenter, G. (1993). The carboxyl terminus of epidermal growth factor/erbB2 chimerae is internalization impaired. *Oncogene* **8**, 3021-3028.
Soubeyran, P., Kowanetz, K., Szymkiewicz, I., Langdon, W. Y. and Dikic, I. (2002). Cbl-CIN85-endophilin complex mediates ligand-induced downregulation of EGF receptors. *Nature* **416**, 183-187.
Stang, E., Blystad, F. D., Kazacic, M., Bertelsen, V., Brodahl, T., Raiborg, C., Stenmark, H. and Madshus, I. H. (2004). Cbl-dependent ubiquitination is required for progression of EGF receptors into clathrin-coated pits. *Mol. Biol. Cell* **15**, 3591-3604.
Stenmark, H., Parton, R. G., Steele-Mortimer, O., Lutcke, A., Gruenberg, J. and Zerial, M. (1994). Inhibition of Rab5 GTPase activity stimulates membrane fusion in endocytosis. *EMBO J.* **13**, 1287-1296.
Stern, D. F., Heffernan, P. A. and Weinberg, R. A. (1986). p185, a product of the neu proto-oncogene, is a receptorlike protein associated with tyrosine kinase activity. *Mol. Cell. Biol.* **6**, 1729-1740.
Tikhomirov, O. and Carpenter, G. (2000). Geldanamycin induces ErbB-2 degradation by proteolytic fragmentation. *J. Biol. Chem.* **275**, 26625-26631.
Tikhomirov, O. and Carpenter, G. (2001). Caspase-dependent cleavage of ErbB-2 by geldanamycin and staurosporin. *J. Biol. Chem.* **276**, 33675-33680.
Volpicelli, L. A., Lah, J. J. and Levey, A. I. (2001). Rab5-dependent trafficking of the m4 muscarinic acetylcholine receptor to the plasma membrane, early endosomes, and multivesicular bodies. *J. Biol. Chem.* **276**, 47590-47598.
Vonderheit, A. and Helenius, A. (2005). Rab7 associates with early endosomes to mediate sorting and transport of Semliki forest virus to late endosomes. *PLoS Biol.* **3**, e233.
Wang, L.-H., Rothberg, K. G. and Anderson, R. G. W. (1993). Mis-assembly of clathrin lattices on endosomes reveals a regulatory switch for coated pit formation. *J. Cell Biol.* **123**, 1107-1117.
Wang, Z. and Moran, M. F. (1996). Requirement for the adapter protein GRB2 in EGF receptor endocytosis. *Science* **272**, 1935-1939.
Wang, Z., Zhang, L., Yeung, T. K. and Chen, X. (1999). Endocytosis deficiency of epidermal growth factor (EGF) receptor-ErbB2 heterodimers in response to EGF stimulation. *Mol. Biol. Cell* **10**, 1621-1636.
Waterman, H., Sabanai, B., Geiger, B. and Yarden, Y. (1998). Alternative intracellular routing of ErbB receptors may determine signaling potency. *J. Biol. Chem.* **273**, 13819-13827.
Waterman, H., Alroy, I., Strano, S., Seger, R. and Yarden, Y. (1999). The C-terminus of the kinase-defective neuregulin receptor ErbB-3 confers mitogenic superiority and dictates endocytic routing. *EMBO J.* **18**, 3348-3358.
Way, T. D., Kao, M. C. and Lin, J. K. (2004). Apigenin induces apoptosis through proteasomal degradation of HER2/neu in HER2/neu-overexpressing breast cancer cells via the phosphatidylinositol 3-kinase/Akt-dependent pathway. *J. Biol. Chem.* **279**, 4479-4489.
Xu, W., Mimnaugh, E., Rosser, M. F., Nicchitta, C., Marcu, M., Yarden, Y. and Neckers, L. (2001). Sensitivity of mature ErbB2 to geldanamycin is conferred by its kinase domain and is mediated by the chaperone protein Hsp90. *J. Biol. Chem.* **276**, 3702-3708.
Xu, W., Marcu, M., Yuan, X., Mimnaugh, E., Patterson, C. and Neckers, L. (2002). Chaperone-dependent E3 ubiquitin ligase CHIP mediates a degradative pathway for c-ErbB2/Neu. *Proc. Natl. Acad. Sci. USA* **99**, 12847-12852.
Yang, X. L., Xiong, W. C. and Mei, L. (2004). Lipid rafts in neuregulin signaling at synapses. *Life Sci.* **75**, 2495-2504.
Yarden, Y. and Sliwkowski, M. X. (2001). Untangling the ErbB signalling network. *Nat. Rev. Mol. Cell. Biol.* **2**, 127-137.
Zhang, F., Crise, B., Su, B., Hou, Y., Rose, J. K., Bothwell, A. and Jacobson, K. (1991). Lateral diffusion of membrane-spanning and glycosylphosphatidylinositol-linked proteins: Toward establishing rules governing the lateral mobility of membrane proteins. *J. Cell Biol.* **115**, 75-84.
Zhou, P., Fernandes, N., Dodge, I. L., Reddi, A. L., Rao, N., Safran, H., DiPetrillo, T. A., Wazer, D. E., Band, V. and Band, H. (2003). ErbB2 degradation mediated by the co-chaperone protein CHIP. *J. Biol. Chem.* **278**, 13829-13837.
Zhou, W. and Carpenter, G. (2001). Heregulin-dependent translocation and hyperphosphorylation of ErbB-2. *Oncogene* **20**, 3918-3920.
Zurita, A. R., Crespo, P. M., Koritschoner, N. P. and Daniotti, J. L. (2004). Membrane distribution of epidermal growth factor receptors in cells expressing different gangliosides. *Eur. J. Biochem.* **271**, 2428-2437.